Available online at www.sciencedirect.com
ScienceDirect
International Journal of Pharmaceutics 349 (2008) 212–225
INTERNATIONAL JOURNAL OF PHARMACEUTICS
www.elsevier.com/locate/ijpharm

Pharmaceutical Nanotechnology

S-Propranolol imprinted polymer nanoparticle-on-microsphere composite porous cellulose membrane for the enantioselectively controlled delivery of racemic propranolol

Chutima Jantarat [a], Naruedom Tangthong [a], Sarunyoo Songkro [a], Gary P. Martin [b], Roongnapa Suedee [a,*]

[a] *Molecular Recognition Materials Research Unit, Department of Pharmaceutical Chemistry, Faculty of Pharmaceutical Sciences, Prince of Songkla University, Hatyai, Songkla 90112, Thailand*
[b] *Pharmaceutical Science Division, Franklin-Wilkins Building, King's College London, London SE1 9NH, UK*

Received 6 April 2007; received in revised form 25 May 2007; accepted 22 July 2007
Available online 31 July 2007

Abstract

Molecularly imprinted polymer (MIP) nanoparticle-on-microspheres (NOM) selective for *S*-propranolol were successfully prepared using suspension polymerization involving agitation of the reaction mixture at high speed. The integration of the MIP-NOM into a self-assembled porous cellulose membrane allowed a controlled distribution and availability of the molecule recognition sites within a porous structure. The nature of the membrane-included microparticles determined the degree of porosity whilst the adherent nanoparticles provided an increased surface area enabling the composite membrane to be employed efficiently for the trans-membrane transport of the imprinted molecule. The MIP-NOM within the membrane were easily accessible for binding of the imprinted molecule and appeared to maintain high selectivity, indicating that the composite membranes may potentially provide valuable affinity matrices. In this study, the application for MIP-NOM composite cellulose membranes were investigated for their potential to act as transdermal drug delivery systems for the *S*-enantiomers from racemic propranolol, its ester prodrugs (cyclopropanoyl- and valeryl-propranolol) or other β-blockers (pindolol and oxprenolol). The enantioselective release of the fluorescently active 1-pyrene-butyryl ester prodrug of *S*-propranolol from MIP-NOM composite membranes and its diffusion and transit across excised rat skin was monitored by confocal laser scanning microscopy. The mechanism underlying the release of *S*-propranolol from the MIP-NOM composite membrane was found to involve specific adsorption and mobility of this enantiomer at the binding site in the MIP-NOM as the latter undergo a transition from the dry to wet state. The proposed MIP-NOM composite membrane controlled release system may be applicable for fabrication of novel membranes with self-controllable permeability responding to the presence of target solutes.

Keywords: Molecularly imprinted polymer; Nanoparticle; Composite membrane; Propranolol; Transdermal delivery

1. Introduction

The recent advent of interest in nanotechnology, has confirmed that particles, liposomes and micelles of the appropriate dimension have a huge potential utility as drug-carriers. Nanotechnology can also be employed to produce molecularly imprinted polymers (MIPs) which may be used as important 'recognition' materials in the construction of biosensors, drug delivery technology or the development of novel separation phases. MIPs can be viewed as synthetically derived artificial receptors that can be formed in the presence of a molecule, the latter being extracted after formation of the polymer, leaving complementary cavities behind *in situ* (Komiyama et al., 2003). MIP materials have been widely studied for their potential role in drug delivery. For example, MIPs have been investigated as base excipients in controlled release devices for theophylline (Alvarez-Lorenzo and Concheiro, 2004) and also in systems devised for the oral and transdermal administration of propranolol (Allender et al., 2000). MIPs with selectivity for timolol have been fabricated into soft contact lenses for timolol-controlled release (Hiratani and Alvarez-Lorenzo, 2002). Moreover the potential use of MIPs has been extended

* Corresponding author. Tel.: +66 74 428239; fax: +66 74 288862.
E-mail address: roongnapa.s@psu.ac.th (R. Suedee).

0378-5173/$ – see front matter © 2007 Elsevier B.V. All rights reserved.
doi:10.1016/j.ijpharm.2007.07.030

to the enantioselective controlled drug delivery of chiral drugs such as β-blockers and non-steroidal anti-inflammatory drugs (NSAIDs) via both the oral and dermal routes (Suedee et al., 2002a,b; Bodhibukkana et al., 2006).

Conventionally, most studies have involved the preparation of MIP particles with a heterogeneous morphology and a resultant broad population of binding sites, which have restricted their functionality in certain applications. MIP particles have been integrated with polymers to form composite membranes but commonly permeability and binding site accessibility can be low due to the close packing of the particles. In addition MIP particles with a very large size are not suitable for obtaining a rapid separation of the imprinted substrate from related compounds as such particles allow only low mass transfer. In contrast, the generation and use of a monodisperse MIP in a composite membrane provides a promising approach for obtaining a reproducible flow distribution through the matrix (Ulbricht, 2004). The regular shape of the MIP micro/nano-particles with a large surface area also allows a more efficient binding of the template molecule to the MIP. Such MIP micro/nano-particles can be engineered either by a suspension polymerization (Mayes and Mosbach, 1996) or precipitation polymerization (Ciardelli et al., 2006). Despite the synthetic methods being straightforward in principal, the final particle size of the generated specific MIPs has often proved difficult to control. Hence the production of the MIP particles and their integration or association with membranes to form a membrane or composite membrane such that the final membrane has a high selectivity (due to the availability of a large number of recognition sites) but with good permeability often proves challenging. A number of different strategies have been proposed to produce MIP-based membranes and a number of the developed methods can involve both the simultaneous formation of MIP sites and the formation of a self-supported membrane with an appropriate morphology. Other technologies have also evolved to incorporate pre-formed MIP particles with or into membranes and these include: coating MIP particles onto the surface of membrane disc (Ciardelli et al., 2006), encapsulation of MIP nanoparticles between two membrane layers (Lehmann et al., 2002), pore-filling of thin track-etched membranes with MIP (Ulbricht et al., 2002), surface grafting of the MIP onto the membrane pores by photoinitiation polymerization (Hattori et al., 2004) and encapsulation of MIP nanoparticles into a composite nanofiber membrane by electrospinning (Chronakis et al., 2006). Clearly the method employed influences the degree of resultant membrane selectivity and influences also its resultant applicability.

Cellulose acetate (Ramamoorthy and Ulbricht, 2003), polysulfone (Yoshikawa et al., 2006), and polyamide (Lehmann et al., 2002) are polymers often exploited as a membrane base for the production of MIP membranes. However, such synthetic membranes are not always suitable for use *in vivo* as a consequence of biocompatibility issues or unsuitable physical properties. In contrast bacterial cellulose (BC), a natural polysaccharide, has been identified as a promising material for use in medical care since it can be produced with high purity, has a high-water binding capacity, high-mechanical strength, and is biodegradable (Klemm et al., 2001). BC can be easily produced by the incubation of *Acetobacter* sp. such as *Acetobacter xylinum* in coconut juice or in any other fruit juices. Such BC is therefore produced in vast amount at a low unit cost from readily available renewable resources found in Southeast Asian countries such as the Philippines, Indonesia, Thailand and Malaysia. These advantages render BC suitable as a possible membrane base for preparing MIP composite membranes for medical application.

Methacrylic acid and ethylene methacrylic acid ester that were the compounds of interest employed in this study, as the monomers for preparation of MIP are found to have biocompatibility and non-toxicity. Since poly(methacrylic acid) and polyethylene glycol (PEG)-based polymers are also used for producing pharmaceutical products such as pharmaceutical tablets, capsules, confectionary or food with water-based ingestible. Methacrylic acid-methacrylic acid ester copolymer with the trademark "Eudragit" is widely used as enteric polymer in controlled drug delivery (Devine et al., 2006; Smith et al., 2006). Moreover, poly(*N*-vinylpyrrolidinone) crosslinked with ethylene glycol dimethacrylate showed biocompatibility and could stimulate fibroblast viability of skin cell (Smith et al., 2006). The methacrylic acid-based polymers exhibited no cytotoxic effects on the caco-2 cell cultures (Torres-Lugo et al., 2002; Foss and Peppas, 2004).

Propranolol, one of the most widely prescribed β-blockers in the long-term treatment of hypertension and cardiovascular diseases is usually taken orally, although an intravenous form is available for acute administration. Propranolol is rapidly absorbed from gastrointestinal tract, but the oral bioavailability is low (∼30%) due to significant first pass metabolism. Propranolol possesses one chiral center and the *S*-isomer is 100–130 times as active as its *R*-isomer (Barrett and Cullum, 1968). There are many racemic compounds which are easily synthesized and which can be simply resolved into their respective enantiomers by using a number of techniques, such as crystallization and preparative high-pressure liquid chromatography. However, the resultant optically pure enantiomer is not always stable and racemization of the drug during pharmaceutical processing and/or storage can often occur. An alternative approach might therefore be to develop a delivery system which allows stereoselective release of a drug. Such a strategy might enable synthetic costs to be controlled, since these are generally higher if the optically pure enantiomer is required. Transdermal controlled drug delivery provides a possible route propranolol administration, but transdermal absorption of propranolol is poor, although a number of different approaches have been investigated with a view to improving permeation (Stott et al., 2001; Namdeo and Jain, 2002; Amnuaikit et al., 2005). Thus, if the *S*-enantiomer of propranolol were to be selectively transported across the skin, a better therapeutic response might be expected relative to that obtained using a racemic mixture of the drug.

The aim of the current study was to seek to produce self-assembled composite porous cellulose membranes containing MIP particles. It was planned to employ a phase inversion technique with the use of polycapolactone-triol as plasticiser. Initial design objectives included the requirement that there should be a high accessibility of the template molecule (the *S*-enantiomer of propranolol) to the binding sites on MIP particles and a high per-

meability of the resultant membrane. The mechanical properties of any formed MIP-containing BC membrane and the latter's enantioselectivity would be studied. Finally it was planned to investigate the enantioselective transport of propranolol (and its prodrugs) across excised rat skin. It was thought that Confocal Laser Scanning Microscope (CLSM) might provide a useful tool for this purpose.

2. Experimental

2.1. Materials

Methacrylic acid (MAA), ethylene glycol dimethacrylate (EDMA) and perfluoro(methylcyclohexane) (PMC) were purchased from Sigma–Aldrich (Milwaukee, WI, USA). MAA was distilled under vacuum before used. EDMA was washed with 1 M aqueous sodium hydroxide and dried over Na_2SO_4 and distilled under vacuum prior to use. 2-(*N*-Ethylperfluorooctane sulfonamide) ethylacrylate (PFA) and 2,2′-azobis-(isobutyronitrile) (AIBN) were supplied by Janssen (Geel, Belgium). The perfluoro polymeric surfactant (PFPS) comprising of 95% acryloyl-2-*N*-ethylperfluoroalkylsulfonamide (PFA) and 5% acryloyl PEG2000 monomethyl ether (PEG2000MME) was prepared, according to the method described by Mayes and Mosbach (1996). *N*-Methylmorpholine-*N*-oxide (NMMO), polycaprolactone-triol (PCL-T), *RS*-propranolol HCl, *S*-propranolol HCl, *RS*-pindolol and *RS*-oxprenolol were purchased from Sigma–Aldrich (Milwaukee, WI, USA). All solvents were analytical grades and dried with molecular sieves to eliminate traces of water before use. Cyclopropanoyl propranolol and valeryl propranolol were prepared by esterification of the racemic propranolol hydrochloride with the acid chloride of the fatty acid, as described previously (Quigley et al., 1994). BC sheet was purchased locally in Songkhla, Thailand, under the Thai government's project "One Tombon, One Product" program (a government sponsored economic development program). The weight of the BC sheet was 273.33 ± 32.14 μg/cm^2 ($n = 3$) and the thickness was 20–30 μm (as measured by SEM).

2.2. Synthesis of the imprinted polymer particles

2.2.1. Granules

The MIP granule, specific for *S*-propranolol was prepared by using thermal polymerization using MAA as a functional monomer, EDMA as a cross-linking monomer and AIBN as a radical initiator and chloroform as a porogen solvent. The print molecule (*S*-propranolol as free base) (2 mmol) was first dissolved in chloroform (15 ml) before the addition of MAA (8 mmol), EDMA (0.05 mol) and AIBN (0.7 mmol). The polymerizing mixture was then degassed under vacuum for 5 min and purged with nitrogen gas for 5 min. The polymerization was performed by oven-heating the mixture at 60 °C for 24 h. The polymer matrix obtained was crushed with a pestle and mortar and sieved through a 100 mesh-sieve (that has sieve opening of 150 μm). The print molecule was extracted from the polymer particulates by sequential washing with 1:9 (v/v) acetic acid and methanol mixture (500 ml, three times) followed by washing with methanol (500 ml, three times) until no residue of print molecule was found in the rinses, as verified by HPLC analysis (see Section 2.8). The resultant polymer was dried under vacuum for 24 h and stored at ambient temperature. Non-imprinted polymer (NIP), which was used as a control to determine selectivity of the MIP, was prepared in the same procedure as the MIP but no template molecule was included in the reaction mixture.

2.2.2. Bead microspheres and nanoparticle-on-microspheres

Bead MIP microspheres were prepared by a suspension polymerization method according to the procedure described by Mayes and Mosbach (1996), involving the use of the perfluoro polymeric surfactant (PFPS) as emulsifier and the perfluoro (methylcyclohexane) (PMC) as dispersing phase. In the typical production procedure of MIP microspheres, MAA (1.6 mmol), EDMA (9.2 mmol), *S*-propranolol (0.4 mmol), AIBN (0.04 mmol), PFPS (25 mg) and PMC (20 ml) were added to chloroform (5 ml). The resultant microemulsion was placed in a 60 ml borosilicate tube (2.5 cm in diameter) and stirred using a rotating blade (30 cm in length and 0.9 cm in diameter) operated at a constant rotation rate (250 rpm). The microspheres were obtained by polymerization involving the irradiation of the stirred mixture with UV light for 4 h at wavelength of 365 nm at room temperature under gentle nitrogen stream. The resulting beads were filtered and the remaining print molecule in the polymer was removed using the same procedure as the granules. The bead microspheres were then dried in vacuum for 24 h and stored at ambient temperature.

The novel MIP nanoparticle-on-microspheres (NOM), first reported here, were prepared by using the same method as for the generation of the bead microspheres but employing a different agitation method, i.e. the use of a magnetic bar instead of a rotating blade, as applied in the Mayes and Mosbach procedure. Thus the production of MIP-NOM involved the use of the same polymerizing composition same as described for the preparation of the bead microspheres. The reaction solution, within a 120-ml vial (5 cm in diameter) was purged with nitrogen gas stream for 5 min. The mixture was vigorously stirred using a 4 cm × 1 cm magnetic bar and a magnetic stirrer set at 1000 rpm. Polymerization of the mixture was again effected by irradiation for 4 h using UV light with a wavelength set at 365 nm.

The stability of the template molecule during the polymerization procedure was determined by measuring the amount of *S*-propranolol that remained in solution after incubation of the drug in chloroform under UV for 4 h. The amount remaining as intact *S*-propranolol was $97.59 \pm 3.90\%$ ($n = 3$). After polymerization, the template molecule was removed by centrifuging the formed MIP-NOM with three portions of 1:9 (v/v) acetic acid and methanol mixture (50 ml) and then with a further three portions of methanol (50 ml) at 3000 G for 5 min after each wash, using a HERMLE rotor Z323K model (Wehingen, Germany). The polymer particles were then dried in a vacuum for 24 h and stored at ambient temperature. As controls, matching NIP-NOM were produced using exactly the same synthetic route but omitting the template molecule from the preparation procedure.

2.3. Evaluation of the recognition properties of the MIP particles

The ability of the MIP particles to selective rebind propranolol enantiomers was evaluated using a solid phase extraction procedure. In order to determine the recovery of bound drug enantiomers from aqueous solution, four different weights of MIP (2, 5, 10 and 15 mg) and separately, the corresponding NIP granules, microspheres, whether bead or NOM, were incubated in 3 ml of pH 7.4 phosphate buffer saline (PBS) containing 60 μg/ml racemic propranolol HCl at room temperature (30 ± 1 °C) for 12 h. The incubated dispersions were centrifuged at 3000 G for 5 min. The concentration of propranolol enantiomers in the supernatant was determined using the stereospecific HPLC method (see Section 2.8). The amount of each enantiomer bound was calculated from the difference in concentrations before and after incubation. All experiments were run in triplicate.

2.4. Preparation of MIP microparticle-containing composite cellulose membranes

In initial experiments it was found that 3.7%, w/w, cellulose dissolved in 50% aqueous NMMO could incorporate up to 35% MIP granules or 104%, w/w, MIP bead microspheres and still form intact composite membranes. Cellulose sheet (96 mg) was dispersed in an aqueous solution of NMMO (50%, w/w) (5 ml) held initially at a temperature of 60 °C. The suspension was then heated at 80 °C until the cellulose dissolved and a clear, brown, viscous solution was obtained. Subsequently, the mixture of 10 mg of racemic propranolol HCl containing 100 mg of granules or bead microspheres or MIP-NOM was prepared for sample dilution. Hundred milligrams of microparticles (or 35 mg of granules) was then titrated with aliquots of the drug by physical mixing. A mixture of 0.3 ml of PCL-T and the corresponding drug polymer mixture (100 mg for microparticles or 35 mg for granules) were added into the cellulose solution. Drug:polymer ratios of 1:5, 1:20, 1:35, 1:70 and 1:170 were employed for MIP granules and ratios of 1:10, 1:50, 1:100, 1:200 and 1:500 were used when the MIP microspheres or MIP-NOM were incorporated. The resulting suspension was cast into a membrane by pouring the melt into a Petri-dish (10 cm in diameter). After 5 min, generated membranes were transferred into a beaker containing 500 ml distilled water for 12 h. Finally, the membrane with a cross-sectional area of 28 cm^2 was recovered, dried in air overnight and stored open in a dessiccator for until required. The entrapment of racemic propranolol HCl in each of the composite membranes was examined by measuring the drug content in the washing solution derived from the cast membranes ($n = 3$) using an HPLC analysis method (see Section 2.8) and the amount of drug entrapped was obtained by subtracting the amount of drug in the rinse solution from the amount of formulation. The thickness of the prepared membranes varied between 90–100 μm as measured by a SEM (JEOL series JSM 5800LV, CA, USA). The matched NIP composite cellulose membranes containing NIP granules or bead microspheres or NIP-NOM were prepared using the same methodology as the equivalent MIP composite cellulose membranes; with drug being included in the reaction mixture in the same ratios. A blank, cast cellulose membrane either with or without PCL-T was also prepared using the same procedure as that for the preparation of MIP or NIP composite cellulose membranes, but in this instance no polymer particles were included.

2.5. Characterization of composite cellulose membranes

2.5.1. Morphology

The membrane morphology of the various composite membranes, blank cast cellulose membranes, and the original cellulose membrane was examined by SEM (JEOL series JSM 5800LV, CA, USA). The samples were sputter-coated with gold before imaging, using an accelerating voltage of 10 kV. The pore size of membranes was estimated from surface pictures of the membrane obtained by SEM.

2.5.2. Mechanical properties

The mechanical strength of three batches of the composite membranes was measured using a Universal testing machine (Lloyd LRX, Fareham, UK) with an operating load of 100 N. The membrane sample was placed between the grips (2.5 cm in length) of the testing machine and testing was carried out at a rate of 30 mm/min. Tensile strength was calculated according to the equation: tensile strength (kN/cm^2) = max load (kN)/cross-sectional area (cm^2).

2.5.3. Electrical resistance

Membrane resistance measurement, as a measure of the composite membrane porosity, was determined using a short-circuit current technique with a Revision G Voltage-Current Clamp, Model VCC 600 (Harvard Apparatus, CA, USA) according to the procedure described previously (Bodhibukkana et al., 2006). Briefly, the test membrane (1 cm^2) was placed in the measuring cell, and a current was set across the membrane using a potentiostat via an amplifier with high-resistance inputs. A 60 μA current was passed through the membrane and the potential difference, PD (mV) and short circuit current, I_{sc} (A) were recorded simultaneously. The membrane resistance, R_m ($\Omega\,cm^2$) was calculated from PD/I_sc according to the Ohm's law (Martin et al., 1993). All experiments were performed three times independently, using three different batches of the composite membrane, at 25 ± 1 °C.

2.5.4. Friability of membranes

The loss of polymer particles from the composite membrane was examined using friability apparatus (Eraweka Abrasion Tester), operated at a constant speed of 25 ± 1 rpm. Samples from three batches of MIP and corresponding NIP composite membranes were rotated in apparatus until the weight of membrane remained constant (about 30 min). The percentage of microparticle loss from the membrane was calculated according to the following equation:

$$\%\text{friability} = \frac{w_1 - w_2}{w_1} \times 100$$

where w_1 and w_2 is the initial and final weight of membrane, respectively.

In addition, the change in membrane resistance of the composite membrane after each friability test was determined using the method described in Section 2.5.3.

2.6. Release experiments

The test membrane (1.5 cm × 1.5 cm) was soaked in 3 ml of 0.2 M pH 7.4 phosphate buffer saline (PBS), which was stirred at a rate of 250 rpm using a magnetic bar. Samples (200 μl) were withdrawn at appropriate time points between 0–6 h and these were replaced by the same volume of fresh PBS. Each test was carried in triplicate at room temperature (30 ± 1 °C) and the release of each propranolol enantiomer was determined using the stereospecific HPLC method (see Section 2.8). The cumulative amount of each enantiomer release was calculated and plotted as a function of time. The flux (J) of each propranolol enantiomer from the membrane loaded with different ratios of drug:polymer was measured from the best-fit linear slope of graph (over 60–180 min) plotted between the cumulative amount of drug release as a function of time. The diffusion coefficient (D, cm^2/h) was obtained from the equation:

$$D = \frac{Jx^2}{C}$$

where C ($\mu g/cm^3$) is the concentration of propranolol enantiomer inside the membrane and x (cm) is the membrane thickness as measured by SEM.

Control experiments were carried out using the composite cellulose membrane containing NIP particles, in order to examine selectivity of the MIP composite membrane.

2.7. In vitro skin permeation study

Male Wistar rat dorsal skin was used in this study. Dorsal hair was removed by shaving, the skin gently excised using surgical scissors and the subcutaneous tissue and adipose tissue carefully removed. The skin preparations were mounted in a Franz-type diffusion cell and the composite membranes (0.8 cm^2) placed in turn on the surface of the stratum corneum in the donor compartment. PBS (2.5 ml,pH 7.4) filled the receiving compartment and 300 μl of PBS was placed in contact with the membrane surface in the donor compartment. The receptor compartment was maintained at 37 ± 1 °C by an external circulating water-bath and the receptor buffer stirred with a magnetic bar. Samples (200 μl) were collected from receptor fluid at set time intervals up to 48 h and immediately replaced with the same volume of fresh PBS. The amount of each propranolol enantiomer permeated at any time point was determined by HPLC (see Section 2.8). The steady-state flux was measured from the linear portion of the plot of the cumulative amount of drug permeated against time. The steady-state portion of the line was extrapolated to the time axis and the point of intersection was recorded as the lag time.

In addition, the permeation rates of racemic mixtures of propranolol prodrugs (cyclopropanoyl-propranolol and valeryl-propranolol) and other β-blockers (oxprenolol and pindolol) were determined. To ensure that sufficient amount of the drugs permeated into the skin to enable sufficient assay sensitivity, 100 mg of the drugs with 100 mg of NOM particulates were incorporated. The composite cellulose membranes were produced as described in Section 2.4. The entrapment of racemic propranolol, cyclopropanoyl-propranolol, valeryl-propranolol, oxprenolol or pindolol in the obtained composite membrane was found to be about the same in each case (2.1 mg/cm^2).

2.8. Stereospecific HPLC method

The different β-blocker enantiomers and related compounds were determined using the stereospecific HPLC method reported previously (Suedee et al., 2000). Each sample (200 μl) was centrifuged at 6000 G for 5 min prior to analysis. The chromatographic system comprised a Waters 600 HPLC system (Bedford, USA) with Waters 717 plus autosampler equipped with a 486 variable wavelength UV detector connected to Waters 746 integrator. A Chiral-AGP column (150 mm × 3 mm, 5 μm) (ChromTech, UK) was employed with a mobile phase comprising 0.5% 2-propanol in 20 mM ammonium acetate buffer pH 4.1 with the wavelength of the assay set at 290 nm for propranolol and its prodrugs. A mobile phase of 1% 2-propanol in 10 mM sodium acetate buffer pH 4.5 with an assay wavelength of at 273 nm was used for oxprenolol, whilst the corresponding conditions for pindolol were 10% acetonitrile in 10 mM sodium phosphate buffer pH 7.0 and a wavelength of 264 nm. The flow rate was set at 1 ml/min for every analysis.

2.9. Confocal laser scanning microscopy (CLSM) study

Confocal Laser Scanning Microscope (CLSM) was utilized as a tool to investigate the mechanism of enantioselective release of derivatised propranolol from the MIP-NOM composite membrane and the subsequent transport of the enantiomers through excised rat skin (∼230 μm thickness). Both *R*-pyrenebutyryl propranolol (1a) and *S*-pyrenebutyryl propranolol (1b), which were used as the fluorescence model compounds, were synthesized from *R*- (or *S*-)propranolol (free base) and 1-pyrenebutyryl chloride. The latter was obtained by reacting 1-pyrene-butyric acid with thionyl chloride, followed by extraction of the product using chloroform. The resulting residue was recrystallised from hexane affording 1a and 1b as a yellow solid: λ_{max}(DMSO) = 360 nm; IR (KBr) d 1730 cm^{-1} (C=O stretching of carbonyl ester), 1268 cm^{-1} (C–O stretching) and 1103 cm^{-1} (C–O–C stretching); ^{1}H NMR ($CDCl_3$, 500 MHz) d 7.3–8.5 ppm (16H, m, aromH), 4.2 ppm (1H, m, *H*C–$(CH_3)_2$), 4.2 ppm (2H, m, O–CH_2), 3.1 ppm (1H, dd, *H*C–O–C=O) and 1.3 ppm (6H, d, J = 5.9 Hz, N–CH(CH_3)$_2$); ^{13}C NMR ($CDCl_3$, 500 MHz): 179.2 ppm (1C, C=O), 134.3–123.1 ppm (16C, aromC pyrene), 134.5–120.8 ppm (10C, aromC naphthalene), 70.4 ppm (1C, H*C*–O–C=O) and 22.7 ppm (2C, N–CH(*C*H_3)$_2$). HRMS: the molecular peak of 1a and 1b was not obtained.

The stability of the 1a and 1b in 80% DMSO (in water) was investigated both at room temperature (30 ± 1 °C) and at 37 °C, since the compounds were used under these conditions. The results showed that more than 90% content of both the *R*- and *S*-propranolol fluorescent probes were found after 7 days incubation at room temperature. This indicated that the first-order stability constants (K_H) of the *R*- and *S*-probes were 0.032 and 0.026 day^{-1}, respectively. The equivalent K_H values at 37 °C of the *R*-probe and *S*-probes were found to be similar (calculated as 0.036 and 0.029 day^{-1}, respectively) indicating an acceptable stability of the enantiomers under these conditions. The MIP-NOM cellulose membranes containing either the 1a or 1b were prepared by mixing 1 mg of each fluorescent probe enantiomer with 100 mg of MIP-NOM particulate before casting into cellulose membrane by using the same protocol as that for the propranolol loaded membrane (see Section 2.4). The entrapment of 1a (27.85 ± 0.48 μg/cm^2, $n = 3$) and 1b (27.50 ± 0.35 μg/cm^2, $n = 3$) probes in the composite membranes were similar, when examined by the method, used for propranolol or its analogues incorporated within cellulose membranes (see Section 2.7).

The experimental set-up for CLSM measurement was carried out in the same way as the skin permeation study described for propranolol at 37 °C (see Section 2.7), except the receptor phase was filled with 2.5 ml of 80% DMSO in water and 300 μl of 80% DMSO in water was applied to the membrane surface within the donor compartment. The permeation of the propranolol probes was determined at different four time intervals (1, 6, 12 and 24 h). At these time points, the membrane and rat skin were recovered and the fluorescent marker distribution in the membrane and skin layer determined using CLSM. Samples of solution were removed from the donor and receiver compartments and these were analyzed for both the respective propranolol probe and 1-pyrene-butyric acid by a fluorescence microscope (Perkin-Elmer, Beaconsfield, UK). The quantity of propranolol probe and 1-pyrene-butyric acid was examined by reference to a calibration curve. Additionally, sections of skin and membrane were also cut transversely using a cryomicrotome (Leica, Bensheim, Germany) and examined by CLSM. Each experiment was performed three times independently.

A CLSM (Olympus, Japan) equipped with an Ar-ion laser (Olympus Fluoview FV-300) and Olympus-IX 70 inverted microscope and ×10 or ×20 dry objectives were used. Optical excitation was carried out using a wavelength of 488 nm and the fluorescence emission was detected at either 630 nm for both the *R*- and *S*-propranolol probes or 580 nm for the hydrolysis product, 1-pyrene-butyric acid. The membrane samples were scanned in 100 μm sections in the direction from the surface in contact with the donor fluid downwards toward the side that was in contact with the skin. The rat skin samples were scanned from the epidermal side to dermal side in 230 μm sections. All specimens were $x - y$ scanned towards the z direction at a rate of 0.25 s/line. The relative intensity (I/I_0) of fluorescence probe and the average intensity (I) of 1-pyrene-butyric acid were plotted as a function of the depth of membrane and/or skin layer, where I_0 was the fluorescent intensity of the initial membrane (or skin) specimen measured at time zero.

2.10. Statistical analysis

Data were expressed as the mean ± S.D. The Student's *t*-test was applied to determine the significance of any differences.

3. Results and discussion

3.1. Polymer particles synthesis

Fig. 1 shows scanning electron micrograph of MIP particles in the form of (a) granules, (b) bead microspheres and (c) MIP-NOM, respectively. There are appreciable differences in the morphology between the polymer granules and beads and these were clearly dependent upon the methods of polymerization. The monolithic particles obtained after bulk polymerization, followed by grinding and sieving have an irregular, rough morphology with diameters ranging from 15 to 35 μm. Nano-sized imprinted polymer would be expected to provide a large imprinted surface with a high-selective potential due to the small size of the nanoparticle. However, in preliminary studies it was found that polymer nanoparticles prepared in our laboratories were difficult to embed in a composite membrane via phase inversion and subsequent casting. In addition such particles tended to form aggregates that would reduce the available surface area of particles. The advantages of MIP-NOM are that in addition to providing a high accessibility of imprint sites they resolved the handling problems associated with generating and incorporating nanoparticles. The MIP bead microspheres synthesized by suspension polymerization method, involving dispersion of the polymer in a liquid perfluorocarbon (PPF), generated spherical uniformly sized particles with a size range of 50–65 μm, which could be suitable for use as a separation phase in chromatography and/or in solid-phase extraction techniques (Mayes and Mosbach, 1996). Such MIP beads, if packed into a column would be expected to confer a low back pressure and rapid diffusion of the analyte molecule. In the current study, it was found that a vigorous controlled stirring rate carried out during the polymerization process, using either a rotating blade or magnetic stirring bar produced particles with a very different morphology. The technique of emulsion polymerization, involves the monomer having only sparing solubility in the continuous phase, in this case PMC. When initiation occurs in this phase the polymer chain radical generated in reaction medium grows to a certain critical chain length, where upon nucleation into primary particles occurs. However, in addition monomer will coalesce into droplets. The formation of NOM in this study may be explained by the core-shell theory, where the primary particles have a polymer-rich core with little monomer but with an outer surrounding shell layer comprising practically pure monomer (Bataille et al., 1982; Hansen and Ugelstad, 1978, p. 1979). The emulsifier used in this procedure was a preformed-polymer obtained from the grafted copolymerization of PFA acrylate and PEG2000MME acrylate, and this stabilizes and allows the formed composed of MAA-EDMA polymer to grow. The agitation of the polymerizing mixture with magnetic bar at very high speed (~1000 rpm) appeared to induce the formation of nanoparticulate monomer droplets as well as the

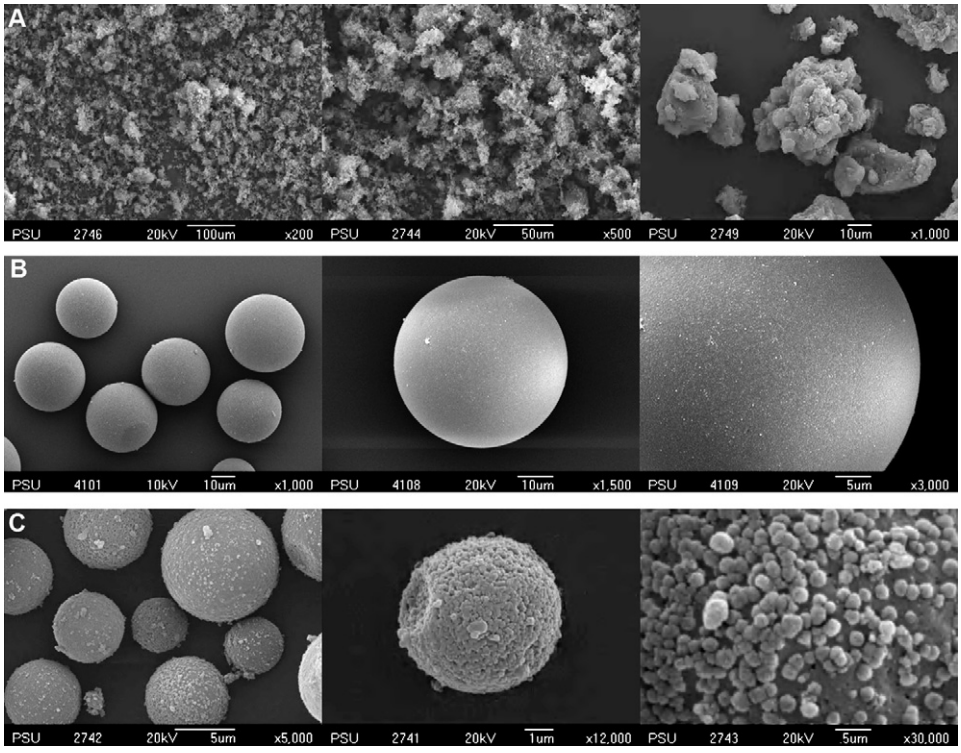

Fig. 1. SEM images of the imprinted polymer particles: granules (A), microspheres (B), nanoparticle-on-microspheres (C).

primary microspheres. As the propagation continues, monomer molecules from the emulsified monomer droplets may diffuse toward the propagating chains within the polymer microspheres. The diffusion of monomer to the polymer nanoparticles also continues at a rapid rate. The polymer particles obtained are in form of uniform nanoparticles, in the size range of 300–500 nm, that are attached onto the surface of microspheres in the size range of 3–10 μm (Fig. 1C).

3.2. Selectivity of propranolol binding to MIP particles

The selective extraction of enantiomer of a fixed concentration of racemic propranolol HCl in pH 7.4 phosphate buffer by increasing amounts of MIP particles was evaluated at room temperature. The enantioselectivity of the binding of propranolol HCl was measured as the amount of each enantiomer bound to the particles expressed as a percentage of the original concentration and this was plotted as a function of polymer content (Fig. 2).

Both MIP- and NIP-granules showed a high % binding of both propranolol enantiomers over the range of polymer content studied. In addition the MIP granules displayed no enantioselectivity of binding. In contrast the binding of both propranolol enantiomers to either the MIP bead microspheres or the MIP-NOM was markedly greater than to the corresponding NIPs. In addition there was clear evidence of enantioselectivity increased as a function of polymer content for the MIP bead microspheres and this was at a maximum when 10 mg polymer was present (or 1:55 drug:polymer ratio). MIP-NOM membranes displayed marked enantioselectivity over the entire range of polymer con-

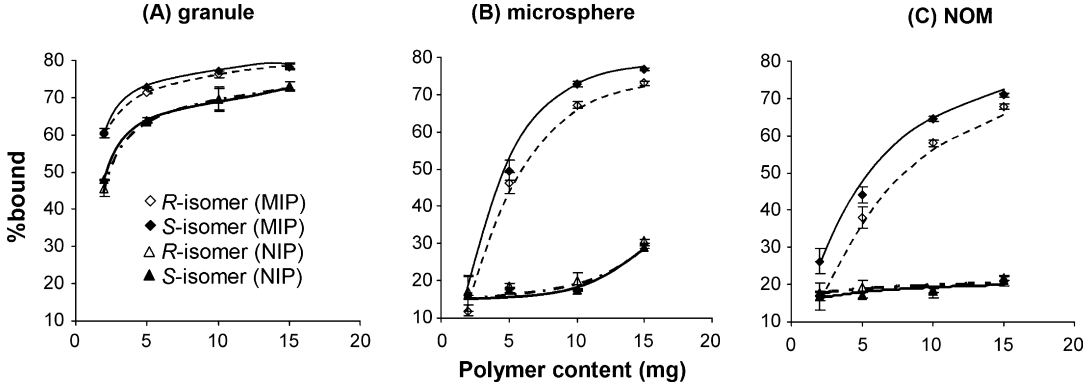

Fig. 2. The percentage of bound propranolol enantiomer after incubation of different weights of imprinted and non-imprinted (A) granule, (B) microsphere and (C) nanoparticle-on-microsphere polymer with 60 μg/ml racemic propranolol in pH 7.4 phosphate buffer solution at room temperature (mean ± S.D., $n = 3$).

tent (2–15 mg) and the degree of enantioselectivity was similar at every level of polymer content. It would appear therefore that the production of granules led to the generation of a material that displayed high non-specific binding sites. In the case of polymer bead microspheres and MIP-NOM, as the polymer content was increased then so the percentage of each enantiomer bound increased significantly. This suggests that the binding sites may be more accessible in the particles produced by emulsification and the increased surface area provided by the MIP-NOM provides an increased efficiency in the rebinding of the template molecule in comparison to the MIP bead microsphere.

3.3. Membrane preparation and characterization

Cellulose does not dissolve in most conventional solvents, due to the strong hydrogen bonds that exist between cellulose chains. However, the latter can be disrupted by *N*-methylmorpholine-*N*-oxide (NMMO) (Fink et al., 2001), the solvent employed in this study. Preliminary experiments were carried out to determine the optimum amounts of components that would enable the production of suitable membranes with respect to appearance and mechanical stability.

Fig. 3 show SEM image of (a) the original cellulose membrane and (b) a cellulose membrane with no added components, after casting. The BC membrane, comprises a porous pellicle (Atalla and Vanderhart, 1984) with good mechanical strength. After casting the BC is converted to a matrix membrane with a smooth surface and a non-porous interior. The mechanical strength of the cast BC membrane (tensile strength = 1.53 kN/cm^2) was markedly lower than that of the original (tensile strength = 3.16 kN/cm^2). However, the swelling properties of the cast BC membrane ($147.50 \pm 24.74\%$) were not significantly different to the original membrane (122.72 ± 6.42 %).

When poly(caprolactone triol) (PCL-T) was added to the BC membrane during phase inversion, then numerous pores were introduced into the matrix (Fig. 3c). The introduction of PCL-T has been reported previously to promote pore formation within polymer membranes (Meier et al., 2004). In this study the BC membrane cast in the presence of PCL-T was more flexible and the tensile strength was lower (1.35 ± 0.13 kN/cm^2) than the BC membrane prepared in the absence of the added component.

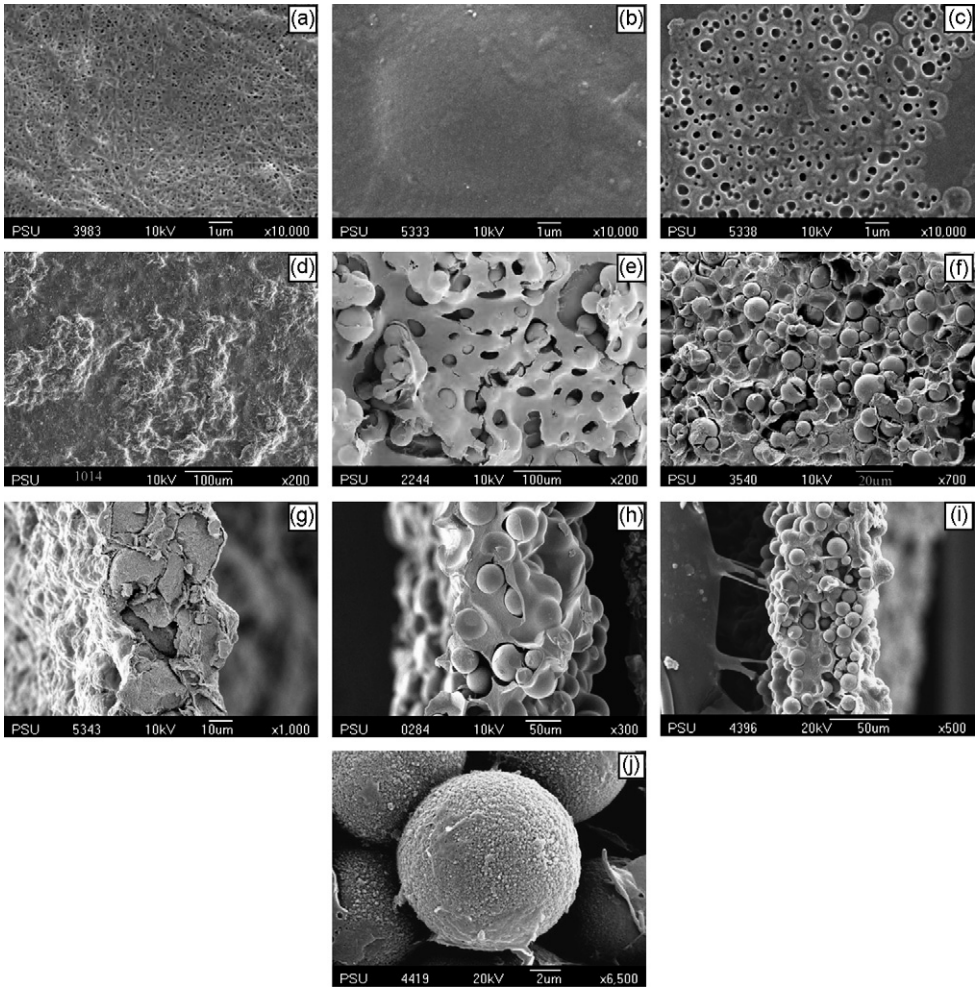

Fig. 3. SEM images of membranes: the original bacterial cellulose (a) blank cellulose cast without the addition of PCL-T, (b) blank cellulose cast with the addition of PCL-T, (c) the MIP granule, MIP microsphere and (d–f) surface, (g–i) cross-section, MIP nanoparticle-on-microsphere (NOM) composite cellulose membranes and (j) the enlargement image of MIP-NOM composite membrane.

Table 1
Characteristics of the composite cellulose membranes for all types of particles

Membrane	Polymer loaded (%)	Pore size (μm)	Membrane resistance (Ω cm^2)	Tensile strength (kN/cm^2)	Friability (%)
Part (A)					
NIP	35	0.40 ± 0.10	1.26 ± 0.42	0.50 ± 0.33	3.11 ± 0.31
MIP	35	0.30 ± 0.05	1.26 ± 0.42	0.25 ± 0.20	2.60 ± 0.19
Part (B)					
NIP	104	42.0 ± 0.04	1.88 ± 0.09	0.72 ± 0.04	1.82 ± 0.37
MIP	104	37.5 ± 0.05	3.13 ± 0.09	0.76 ± 0.03	1.47 ± 0.38
Part (C)					
NIP	104	6.30 ± 2.10	2.95 ± 0.85	0.73 ± 0.14	2.54 ± 0.31
MIP	104	10.5 ± 2.01	2.22 ± 0.92	0.56 ± 0.38	2.70 ± 0.53

(A) Granule; (B): microsphere, (C) NOM containing membrane.

The surface morphology and cross-sectional architecture of BC membranes loaded with MIP granules, bead microspheres or NOM are also shown in Fig. 3(d–i). The SEM images showed that the surface of the membranes that contained particles exhibited a rough appearance. The membrane loaded with beads displayed a higher porosity than the membrane loaded with granules. The pores of composite membranes were induced by PCL-T during the phase inversion preparation procedure. However, the resultant pore size of the composite membranes is partly dependent on the size of the polymer beads size, with the membrane loaded with polymer granules showing low porosity. This may have been due to the bulkiness of the polymer granules coupled with their tendency to form aggregates, which packed in a layer at the bottom of the composite membrane. In case of the MIP-NOM loaded membranes, it was apparent that even after casting of the membrane, the nanoparticles were still visible as being attached on the surface of microsphere (Fig. 3j). This indicates that the nanoparticles are adhered strongly to the microsphere.

The physical properties of the BC composite membranes containing either 35%, w/w, granules or 104%, w/w, microparticles (bead microsphere or NOM) are shown in Table 1. The mechanical strength of the MIP microsphere containing composite membranes was higher than the corresponding granule and NOM composite membranes. The pore size of granule containing composite membrane was markedly smaller than either the microsphere or NOM containing composite membranes. The microsphere containing membrane displayed the largest pore size, due to the integrated particles having the largest particle size. These results confirm the visual findings apparent from the SEM images (Fig. 3).

The microsphere-containing membranes were less friable than the granule or NOM containing membranes. The electrical resistance of the membranes was redetermined, after the friability test had been carried out but this was found to change less than 2.5% in all cases. All the composite membranes retained a good appearance after testing and it was concluded that all membranes would have sufficient robustness for experimental application purposes.

3.4. Drug release

The diffusion coefficient of both propranolol enantiomers and the enantioselectivity of the various MIP-containing BC membranes were dependent upon the drug:polymer ratio (Fig. 4). It was also apparent that both parameters (i.e. diffusion coefficient and enantioslectivity) were dependent upon the configuration of MIP particle. Thus when the cumulative amount of the individual propranolol enantiomers released was plotted as a function of time then the profiles obtained were membrane dependent, as was the inherent stereoselective release (Fig. 5). The cumulative release from the corresponding NIP membranes was also determined for comparison purposes. The diffusivity of the drug was higher from membranes containing the MIP microspheres or MIP-NOM, due to the higher porosity of these two membranes in comparison to the BC containing

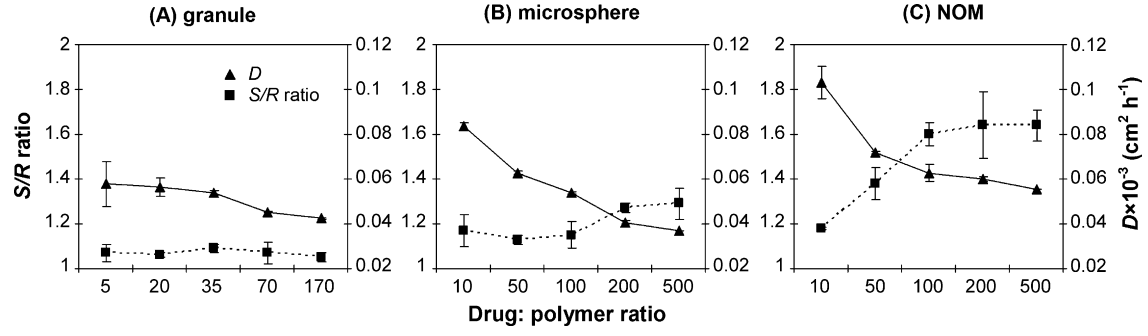

Fig. 4. The diffusion coefficient (*D*) of *R*- and *S*-propranolol and the *S*/*R* ratio obtained from permeation study by using Franz-diffusion cell of (A) MIP granule- (B) MIP microsphere- and MIP (C) nanoparticle-on-microsphere-contained in composite bacterial cellulose membranes at various polymer loadings after incubation in pH 7.4 phosphate buffer and room temperature (mean ± S.D., $n = 3$).

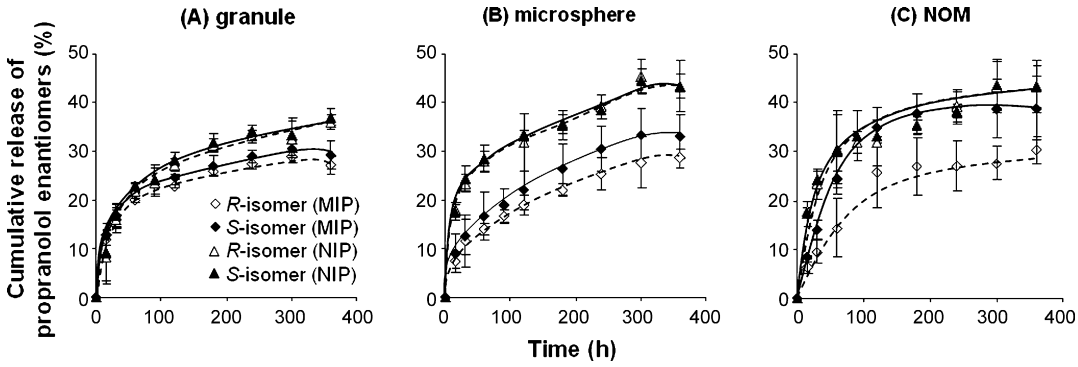

Fig. 5. The release profiles of propranolol enantiomers from molecularly imprinted and non-imprinted polymers of (A) granule, (B) microsphere and (C) nanoparticle-on-microsphere composite bacterial cellulose membranes at the drug:polymer loading ratios of 1:35 for the granule and 1:100 for microsphere and nanoparticle-on-microsphere membranes. The experiment was performed by applying pH 7.4 phosphate buffer as medium to the membranes at room temperature (mean ± S.D., $n = 3$).

MIP granules. And, the diffusivity of propranolol molecules in membranes containing the MIP-NOM was greater than in membranes containing the MIP microspheres for the equivalent drug:polymer ratios (Fig. 4). This apparent discrepancy has been interpreted as an indication of a more even flow distribution of the NOM loaded membrane. The total amount of drug incorporated in each of the MIP composite cellulose membrane and the matched NIP composite cellulose membrane of granule, microsphere and nanoparticle-on-microsphere at various drug:polymer ratios was displayed in Table 2. The amount of *R*- and *S*-propranolol enantiomers incorporated in the MIP composite membranes and the matched NIP composite membrane was not significantly different for the equivalent drug:polymer ratios. Also, there was no stereoselective difference in the amount of propranolol enantiomers entrapped in the MIP or the matched NIP composite membranes. As shown in Fig. 5, both *R*- and *S*-propranolol enantiomers were transported faster through the matched NIP composite membranes than though the MIP composite membranes, except the MIP-NOM containing membrane showed the release of *S*-isomer similar to the NIP-NOM containing membrane. The resulting curves indicate that the diffusion of *R*-propranolol across the MIP composite membranes is delayed whereas a relatively facilitated transport of *S*-propranolol across MIP membranes. The preferential sorption of *S*-propranolol to MIP granules and microparticles enhances the transport selectivity of the MIP composite membranes. Enantioselective release was obtained from all three BC composite membranes, with the *S*-propranolol enantiomer being released preferentially in comparison to the *R*-propranolol enantiomer. However, the membrane containing NOM showed the highest enantioselectivity compared to the other membranes which incorporated propranolol at the same

Table 2
The entrapment of propranolol enantiomers in the membrane loaded with different drug:polymer ratios (mean ± S.D., $n = 2$)

Drug:polymer ratio	Entrapment (μg/cm^2)			
	NIP-membrane		MIP-membrane	
	R-isomer	*S*-isomer	*R*-isomer	*S*-isomer
Part (A)				
1:5	104.2 ± 10.2	106.0 ± 9.0	104.6 ± 9.0	106.0 ± 10.2
1:20	20.8 ± 2.0	21.2 ± 1.8	19.9 ± 1.8	21.2 ± 2.8
1:35	9.9 ± 1.4	9.9 ± 0.9	10.4 ± 1.0	10.6 ± 0.9
1:70	5.0 ± 0.3	5.2 ± 0.5	4.9 ± 0.4	5.0 ± 0.4
1:170	2.4 ± 0.2	2.6 ± 0.3	2.6 ± 0.3	2.6 ± 0.2
Part (B)				
1:10	111.1 ± 11.3	111.5 ± 5.8	106.9 ± 10.0	106.4 ± 5.8
1:50	21.2 ± 1.4	21.2 ± 2.6	22.0 ± 2.3	20.5 ± 2.5
1:100	10.2 ± 1.0	10.3 ± 0.8	10.6 ± 1.1	10.6 ± 1.2
1:200	5.3 ± 0.6	5.3 ± 0.3	5.3 ± 0.3	5.3 ± 0.2
1:500	2.7 ± 0.1	2.6 ± 0.3	2.6 ± 0.1	2.8 ± 0.1
Part (C)				
1:10	108.6 ± 7.8	109.0 ± 11.0	106.2 ± 7.0	109.7 ± 5.2
1:50	19.9 ± 0.9	19.8 ± 0.8	20.8 ± 1.0	21.2 ± 1.5
1:100	9.3 ± 0.3	9.6 ± 0.4	11.0 ± 0.9	10.6 ± 0.5
1:200	5.3 ± 0.3	4.9 ± 0.3	5.3 ± 0.3	5.3 ± 0.2
1:500	2.7 ± 0.2	2.5 ± 0.1	2.4 ± 0.1	2.8 ± 0.1

(A) Granule, (B) microsphere, (C) NOM containing membrane.

drug:polymer ratios. As the polymer loading increased the diffusivity of both propranolol enantiomers decreased (Fig. 4), but the stereoselectivity increased for the BC membranes containing MIP microspheres or NOM. The greatest enantioselectivity of release from the membrane-containing MIP-NOM was probably as a consequence of the higher surface area of the incorporated particles which allowed good accessibility of the template molecule to the MIP binding sites. The *S*/*R* selectivity of the MIP microparticle composite membranes was increased when the MIP loading was increased but above a drug:polymer ratio of 200 for the microsphere (*S*/*R* flux ratio = 1.2) and at a drug:polymer ratio of 100 for NOM membranes (*S*/*R* flux ratio = 1.7), there was no further increase. These results indicate that the selectivity is likely to be influenced by the capacity of the available MIP particles within the BC membrane to bind the template molecule. In the case of granule-containing composite membranes, as a consequence of the nature of granules, which have a high volume/weight ratio, the MIP could not be loaded into the membrane in the same, higher amounts, as the membrane containing MIP microparticles. The maximum loading of granular MIP was 1:170, drug:polymer. The *S*/*R* selectivity obtained for the granule-loaded membrane did not change with increased polymer loading and a low *S*/*R* selectivity (∼1.1) was obtained for all drug:polymer ratios employed.

The release profiles of *R*- and *S*-propranolol enantiomers from the composite membrane loaded with MIP and NIP granules, microspheres and MIP-NOM at a fixed drug:polymer ratio of 1:35 in the case of granules and 1:100 in the case of microspheres and MIP-NOM, when pH 7.4 phosphate buffer was employed as the diffusing dissolution medium, are shown in Fig. 5. Initially, the drug release was rapid with low enantioselectivity, possibly as a consequence of the drug located at the membrane surface dissolving into the receptor fluid. After the 'burst' release of propranolol, subsequent release of the enantiomers was slower but stereoselectivity was increased. Drug at this stage was presumably being released from the binding sites of MIP in the membrane. Release from the control membranes, containing equivalent NIP particles, showed the release rate of drug to decrease as a function of time in a similar manner to the membranes loaded with MIP particles. However, no enantioselectivity in the release of propranolol was found for all types of NIP particle, whether incorporated as granules or microparticles.

3.5. *In vitro* skin permeation study

The enantiomeric release and the subsequent transdermal transport of propranolol and propranolol prodrugs (isovaleryl-propranolol and cyclopropanoyl-propranolol) as well as other β-blockers (oxprenolol and pindolol) from the MIP-NOM loaded BC membrane *in situ* with excised rat skin was determined (Table 3). The results indicated that the transport of *S*-propranolol across rat skin after release from MIP-NOM composite membranes was higher than the concomitant transport of *R*-propranolol. Also, the transport of the more lipophilic propranolol prodrug enantiomers occurred at a higher rate than that of the parent enantiomers. The transport rates of the *R*- and *S*-enantiomers of the propranolol and its prodrugs were found to be different ($P < 0.05$). The various esterases present in the skin would be expected to act upon the prodrug during its transport through the viable epidermis and dermis. The rate of hydrolysis of isovaleryl-propranolol and cyclopropanoyl-propranolol within the rat skin has been reported to be enantiomer dependent, with that *R*-isomer enantiomer prodrug being hydrolyzed faster than *S*-isomer prodrug (Ahmed et al., 1997). However, no overall difference was apparent in the extent of enantioselectivity of transport of either of the propranolol prodrugs, nor indeed when the degree of enantioselectivity of the prodrugs was compared to that obtained for propranolol itself. The MIP-NOM BC composite membrane also produced statistically significant differences in the fluxes of the oxprenolol and pindolol enantiomers ($P < 0.05$). The results obtained indicate that there was a cross-reactivity between the *S*-propranolol imprinted MIP-NOM and compounds that are structurally related to the template. Nevertheless, no enantioselectivity was detected in the lag times determined for the diffusion through skin for any of the racemic compounds studied.

Table 3
In vitro rat skin permeation data of racemic propranolol, prodrugs of propranolol and other β-blockers release from MIP and NIP nanoparticle-on-microsphere loaded bacterial cellulose membranes after application of pH 7.4 phosphate buffer at 37 ± 1 °C (mean ± S.D., $n = 3$)

Drug	Membrane	J_{ss} ($\mu g\,cm^{-2}\,h^{-1}$)[a]			τ (h)[b]		
		R-Isomer	*S*-Isomer	*S*/*R* ratio	*R*-Isomer	*S*-Isomer	*S*/*R* ratio
Propranolol	NIP	0.32 ± 0.06	0.31 ± 0.12	0.95 ± 0.18	28.53 ± 0.46	27.73 ± 0.92	0.97 ± 0.02
	MIP	0.43 ± 0.09	0.57 ± 0.08	1.33 ± 0.18	20.27 ± 6.74	18.13 ± 10.27	0.85 ± 0.19
Cyclopropanoyl-propranolol	NIP	2.17 ± 0.01	1.96 ± 0.03	0.91 ± 0.01	20.50 ± 2.26	20.23 ± 2.70	0.99 ± 0.02
	MIP	8.72 ± 0.07	11.79 ± 0.13	1.36 ± 0.03	20.23 ± 7.43	16.53 ± 6.22	0.81 ± 0.01
Valeryl-propranolol	NIP	4.86 ± 0.92	5.08 ± 0.33	1.05 ± 0.13	13.20 ± 2.11	12.93 ± 1.84	0.98 ± 0.03
	MIP	4.62 ± 0.11	5.87 ± 0.02	1.27 ± 0.02	15.33 ± 2.57	12.00 ± 2.80	0.88 ± 0.03
Oxprenolol	NIP	9.85 ± 3.63	10.44 ± 4.56	1.04 ± 0.14	12.46 ± 3.44	12.73 ± 3.90	1.01 ± 0.03
	MIP	16.77 ± 0.88	19.48 ± 0.69	1.16 ± 0.02	12.60 ± 3.34	11.06 ± 2.72	0.86 ± 0.02
Pindolol	NIP	5.04 ± 0.68	4.91 ± 0.74	0.97 ± 0.01	10.53 ± 0.92	10.46 ± 0.98	0.99 ± 0.01
	MIP	3.83 ± 0.32	4.48 ± 0.26	1.16 ± 0.03	13.46 ± 2.01	11.65 ± 1.60	0.86 ± 0.02

[a] Steady-state transdermal flux.
[b] Lag time.

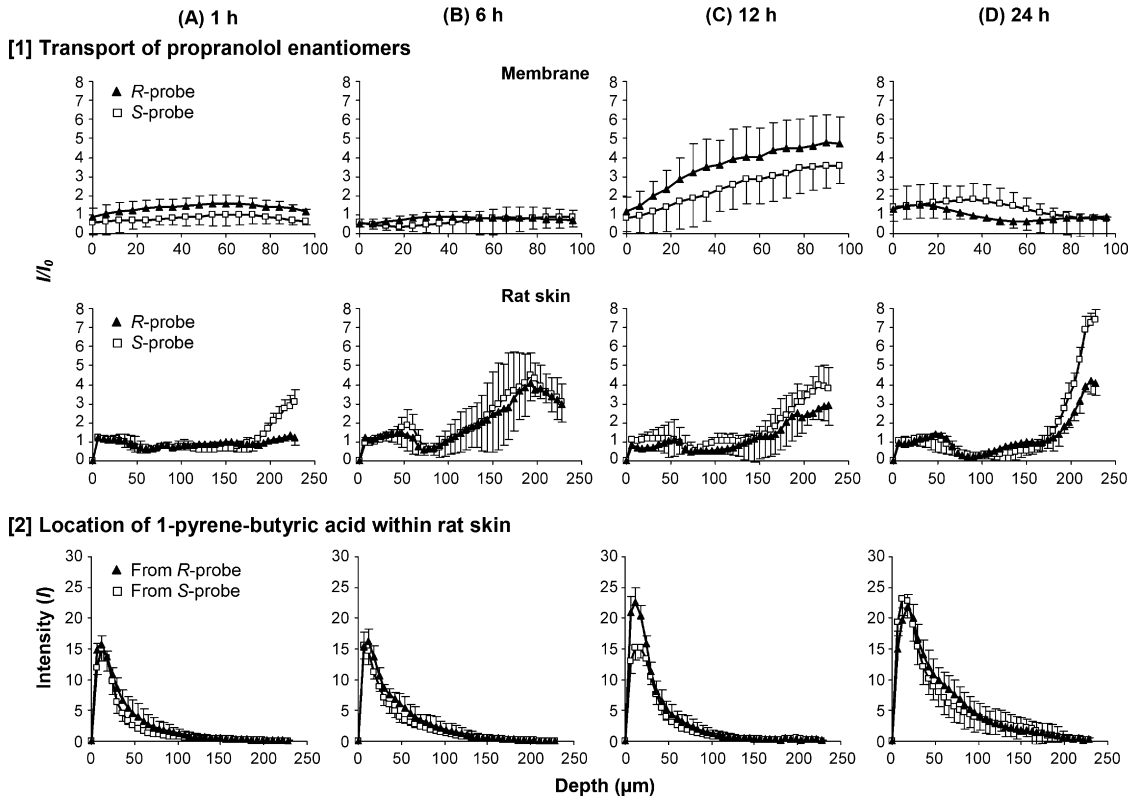

Fig. 6. The relative intensity (I/I_0) of fluorescence and the average intensity (I) of 1-pyrene-butyric acid (the hydrolysis degradation product) plotted against depth (μm) in the membrane and in rat skin after 1, 6, 12 and 24 h of propranolol enantiomer probe transport from the MIP nanoparticle-on-microsphere composite membrane placed onto rat skin sections (mean ± S.D., $n = 3$).

3.6. Confocal laser scanning microscopy study

In order to investigate the mechanism of selective release of the propranolol enantiomers from the MIP-NOM composite BC membrane, the membranes were fabricated in the presence of either the *R*- or *S*-propranolol enantiomer labeled with the 1-pyrene butyric acid probe. It was reported previously that propranolol ester prodrugs were released enantioselectively from a BC membrane which had been grafted to a *S*-propranolol imprinted polymer layer, produced from the same materials as those employed in the present study (Bodhibukkana et al., 2006). In that study the *S*-isomer was released at a faster rate than the *R*-isomer. The intensity of fluorescence emission of the membrane and rat-skin at 630 nm, the wavelength used to monitor the transport of the *R*- and *S*-propranolol esters was found to be very low. The CLSM scan provided a 2-D image of both coupled propranolol probe and 1-pyrene-butyric acid, a product derived from the 1-pyrenebutyryl propranolol enantiomers by hydrolysis effected by enzymes in the skin.

Fig. 6 shows the relative intensity (I/I_0) of the *R*- and *S*-enantiomer of fluorescence probe detected in either the membrane or rat skin layer at different depths after treatment for 1, 6, 12 or 24 h. The amounts of *R*- and *S*-propranolol probe enantiomer detected in donor and receiving phase as well as the amounts of 1-pyrene-butyric acid that was found in rat skin samples at different time points are shown in Table 4. The results showed that mean I/I_0 of either *R*- or *S*-propranolol fluorescent probes at most depths of the membrane after treatment for 1 and 6 h was about 1 and that there was no statistical difference between I/I_0 values of the *R*- and *S*-isomer in the membranes at these time points. A greater amount of the *S*-propranolol fluorescent probe in comparison to *R*-probe was detected in the donor

Table 4
The concentration of *R*- and *S*-propranolol probe and 1-pyrene-butyric acid detected in donor and receiver phases after application of solvent to a membrane placed on isolated rat epidermal sections (mean ± S.D., $n = 3$)

Time (h)	Enantiomer	The probe		1-Pyrene-butyric acid
		Donor (μg/ml)	Receiver (μg/ml)	Receiver (μg/ml)
1	*R*	0.10 ± 0.01	ND	ND
	S	1.52 ± 0.09	ND	ND
	S/*R* ratio	15.51 ± 0.40	ND	ND
6	*R*	0.35 ± 0.04	ND	0.54 ± 0.11
	S	2.59 ± 0.15	ND	0.32 ± 0.20
	S/*R* ratio	7.43 ± 0.96	ND	0.55 ± 0.12
12	*R*	2.25 ± 0.17	1.15 ± 0.28	1.03 ± 0.88
	S	3.53 ± 0.14	1.39 ± 0.63	0.33 ± 0.12
	S/*R* ratio	1.51 ± 0.07	1.34 ± 0.02	0.52 ± 0.05
24	*R*	3.32 ± 0.70	3.05 ± 0.16	2.75 ± 1.32
	S	6.55 ± 0.58	4.78 ± 0.55	1.94 ± 0.19
	S/*R* ratio	2.10 ± 0.77	1.57 ± 0.25	0.76 ± 0.04

ND: non-detectable.

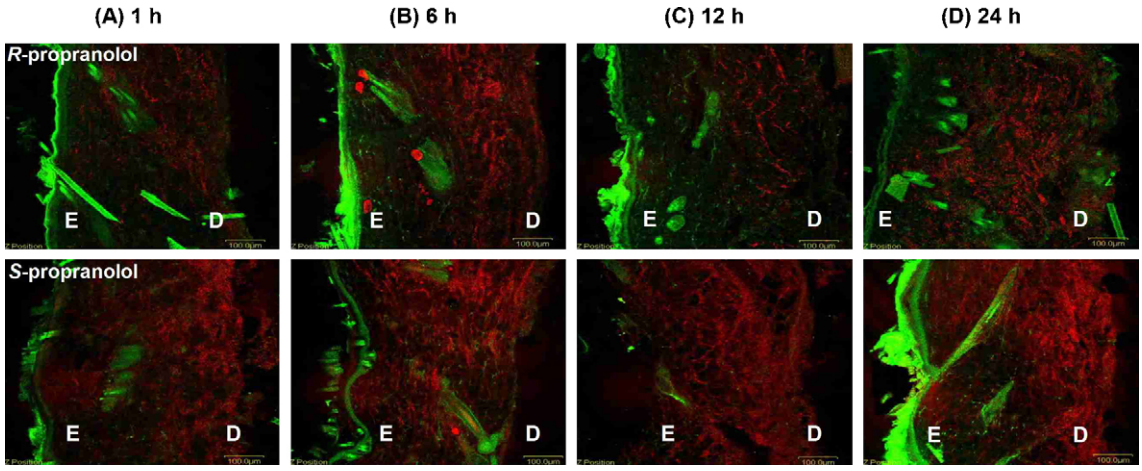

Fig. 7. CLSM image showing distribution of *R*- and *S*-propranolol fluorescent probe (red) in rat skin specimen (cross section) after treatment for 1, 6, 12 and 24 h overlaid with blank (control) rat skin (green); *E* = epidermal side, *D* = dermal side.

solution after 1 and 6 h due to diffusion of the probes from the membrane into the applied donor phase, whilst neither probe was present in the receiving phase after the same time intervals. The diffusion of the probes through the stratum corneum is clearly proceeding during this time (Fig. 6) and after 1 h the *S*-enantiomer can be determined in higher concentration than the *R*-enantiomer in the lower layers of the skin. It was found that the fluorescent intensity of both propranolol analogues within the membrane, 12 h after initial application was markedly greater than that before solvent was applied (Fig. 6). Before treatment of the membrane with solvent the propranolol probes are included in the dry state within the MIP particles in the composite membrane, and this is poorly detected by CLSM. After solvent has diffused into the membrane and the propranolol probes are dissolved the fluorescence can be determined by CLSM. More of the *R*-probe was detected within the membrane after 12 h than the *S*-probe, whilst more *S*-probe was present in the donor phase after this time, having been selectively extracted. At 24 h an *S*/*R* selectivity of permeation into lower skin layers was apparent for the probe, particularly at depths closer to the dermal side. A significantly higher concentration of the *S*-enantiomer had diffused from the membrane across the skin after 24 h in comparison to the *R*-enantiomer (Table 4).

Fig. 7 shows the typical photomicrographs of the distribution of *R*- and *S*-fluorescent probes within rat skin samples after treatment for 1, 6, 12 or 24 h. At all time points the fluorescence from either probe was more apparent within the dermal rather than the epidermal layers. In addition at most time points it was apparent that the intensity of fluorescence of the *S*-propranolol probe within the dermal area of the skin. These observations were confirmed broadly by the measurement of the fluorescent intensity at different levels by CLSM, although no difference was determined experimentally in the fluorescent intensity of the two enantiomeric probes after 6 h (Fig. 6). Enantioselectivity in the release of drug from the membrane appears to be a principal factor in the enantioselective delivery of *S*-propranolol across rat skin. Facilitated release of the template isomer of MIP-NOM occurs after the racemate is loaded into the composite membrane. The mechanism underlying the release of *S*-propranolol from the MIP-NOM composite membrane involves to the non-covalent interaction of this enantiomer with the MIP binding site in the MIP-NOM membrane and disruption of this binding with solvents that causes the release of the isomer into the receiving or donor phases. The binding of *S*-propranolol to the MIP may result in a structural change to the polymer, which perhaps results in polymer shrinkage or swelling, when in the dry or wet state (Suedee et al., 2002a,b). Such a phenomenon might contribute to the increased mobility of *S*-propranolol at the binding site, leading to a more rapid release of this isomer from the membrane.

As discussed previously esterases are present in the skin which will enhance the hydrolysis of a variety of different ester compounds. Some ester prodrugs which are chiral compounds are widely used for the enhancement of percutaneous penetration and these have been reported to show stereoselective hydrolysis in skin (Ahmed et al., 1997). Fig. 6 shows the fluorescence intensity of 1-pyrene-butyric detected at different depths of skin layer after permeation of *R*- or *S*-propranolol probe for 1, 6, 12 or 24 h and, the amount of transport to the receptor compartment after the same time intervals is shown in Table 4. The 1-pyrene-butyric acid is derived from the hydrolysis of the propranolol ester fluorescence probe by the enzymes in rat skin. The hydrolysis of the *R*-propranolol probe was found to be markedly higher than that of the *S*-propranolol at depths between 10-20 μm after 12 h of permeation, but at 24 h the conversion of either *R*- or *S*-enantiomer probes to 1-pyrene-butyric acid was not significantly different (Fig. 6). The rate of hydrolysis of the *R*- and *S*-propranolol probes due to the enzyme in the excised rat skin was calculated as 7.96 and 6.84 day^{-1}, respectively.

4. Conclusions

In this study, the MIP-NOM that was synthesized could be successfully fabricated into a self-assembled porous BC membrane using a phase inversion method. The resultant composite membrane showed enantioselectivity of release for propranolol

enantiomers. Such membranes displayed greater enantioselectivity than membranes containing the same polymer but presented either as granules or microspheres. The increased surface area of the MIP-NOM allowed rebinding of the template molecule to occur more effectively. The MIP-NOM BC composite membrane was employed to show its potential application in the enantioselective-controlled delivery of the *S*-isomer of racemic propranolol and its prodrug analogs through rat skin.

Acknowledgements

Financial support from the Thailand Research Fund through the Royal Golden Jubilee Ph.D. Program (Grant No. PHD/0161/2546) and the NANOTEC Center of Excellence at Prince of Songkla University, Thailand is acknowledged. The authors would like to thank Prof. Franz L. Dickert, the Dean of Institute of Analytical Chemistry, Faculty of Chemistry, University of Vienna for knowledge in fluorescence microscopes.

References

Ahmed, S., Imai, T., Yoshigae, Y., Otagiri, M., 1997. Stereospecific activity and nature of metabolizing esterases for propranolol prodrug in hairless mouse skin, liver and plasma. Life Sci. 61, 1879–1887.

Allender, C.J., Richardson, C., Woodhouse, B., Heard, C.M., Brain, K.R., 2000. Pharmaceutical applications for molecularly imprinted polymers. Int. J. Pharm. 195, 39–43.

Alvarez-Lorenzo, C., Concheiro, A., 2004. Molecularly imprinted polymers for drug delivery. J. Chromatogr. B 804, 231–245.

Amnuaikit, C., Ikeuchi, I., Ogawara, K., Higaki, K., Kimura, T., 2005. Skin permeation of propranolol from polymeric film containing terpene enhancers for transdermal use. Int. J. Pharm. 289, 167–178.

Atalla, R.H., Vanderhart, D.L., 1984. Native cellulose: a composite of two distinct crystalline forms. Science 223, 283–285.

Barrett, A.M., Cullum, V.A., 1968. The biological properties of the optical isomers of propranolol and their effects on cardiac arrythemias. Br. J. Pharmacol. 34, 43–55.

Bataille, P., Van, B.T., Pharm, Q.B., 1982. Emulsion polymerization of styrene. I. Review of experimental data and digital simulation. J. Polym. Sci. Polym. Chem. 20, 795–810.

Bodhibukkana, C., Srichana, T., Kaewnopparat, S., Tangthong, N., Bouking, P., Martin, G.P., Suedee, R., 2006. Composite membrane of bacterially-derived cellulose and molecularly imprinted polymer for use as a transdermal enantioselective controlled-release system of racemic propranolol. J. Contr. Release 113, 43–56.

Chronakis, I.S., Jakob, A., Hagström, B., Ye, L., 2006. Encapsulation and selective recognition of molecularly imprinted theophylline and 17$^{\beta}$-estradiol nanoparticles within electrospun polymer nanofibers. Langmuir 22, 8960–8965.

Ciardelli, G., Borrelli, C., Silvestri, D., Cristallini, C., Barbani, N., Giusti, P., 2006. Supported imprinted nanospheres for the selective recognition of cholesterol. Biosens. Bioelectron. 21, 2329–2338.

Devine, D.M., Devery, S.M., Lyons, L.G., Geever, L.M., Kennedy, J.E., Higginbotham, C.L., 2006. Multifunctional polyvinylpyrrolidinone-polyacrylic acid copolymer hydrogels for biomedical applications. Int. J. Pharm. 326, 50–59.

Fink, H.P., Weigel, P., Purz, H.J., Ganster, J., 2001. Structure formation of regenerated cellulose materials from NMMO-solutions. Prog. Polym. Sci. 26, 1473–1524.

Foss, A.C., Peppas, N.A., 2004. Investigation of the cytotoxicity and insulin transport of acrylic-based copolymer protein delivery systems in contact with caco-2 cultures. Eur. J. Pharm. Biopharm. 57, 447–455.

Hansen, F.K., Ugelstad, J., 1978. Particle nucleation in emulsion polymerisation. I. Theory of homogeneous nucleation. J. Polym. Sci. Polym. Chem. 16, pp. 1953, 1978 (II. Nucleation in emulsifier-free systems investigated by seed polymerization; III. Nucleation in systems with anionic emulsifier investigated by seeded and unseeded polymerization; IV. Nucleation in monomer droplets. J. Polym. Sci. Polym. Chem., 17, pp. 3033, 3047, 3069).

Hattori, K., Hiwatari, M., Iiyama, C., Yoshimi, Y., Kohori, F., Sakai, K., Piletsky, S.A., 2004. Gate effect of theophylline-imprinted polymer grafted to the cellulose by living radical polymerization. J. Memb. Sci. 233, 169–173.

Hiratani, H., Alvarez-Lorenzo, C., 2002. Timolol uptake and release by imprinted soft contact lenses made of *N,N*-diethylacrylamide and methacrylic acid. J. Contr. Release 83, 223–230.

Klemm, D., Schumann, D., Udhardt, U., Marsch, S., 2001. Bacterial synthesized cellulose-artificial blood vessels for microsurgery. Prog. Polym. Sci. 26, 1561–1603.

Komiyama, M., Takeuchi, T., Mukawa, T., Asanuma, H., 2003. Fundamentals of molecular imprinting. In: Molecular Imprinting. Wiley-VCH Verlag GmbH & Co. KGaA, Weinheim, pp. 9-19.

Lehmann, M., Brunner, H., Tovar, G.E.M., 2002. Selective separations and hydrodynamic studies: a new approach using molecularly imprinted nanosphere composite membranes. Desalination 149, 315–321.

Martin, A., Bustamante, P., Chun, A.H.C., 1993. Solution of electrolytes. In: Physical Pharmacy: Physical Chemical Principles in the Pharmaceutical Sciences, fourth ed. LEA & FEBIGER, London, p. 126.

Mayes, A.G., Mosbach, K., 1996. Molecularly imprinted polymer beads: suspension polymerization using a liquid perfluorocarbon as the dispersing phase. Anal. Chem. 68, 3769–3774.

Meier, M.M., Kanis, L.A., Soldi, V., 2004. Characterization and drug-permeation profiles of microporous and dense cellulose acetate membranes: influence of plasticizer and pore forming agent. Int. J. Pharm. 278, 99–110.

Namdeo, A., Jain, N.K., 2002. Liquid crystalline pharmacogel based enhanced transdermal delivery of propranolol hydrochloride. J. Contr. Release 82, 223–236.

Quigley, J.M., Jordan, C.G.M., Timoney, R.F., 1994. The synthesis, hydrolysis kinetics and lipophilicity of O-acyl esters of propranolol. Int. J. Pharm. 101, 145–163.

Ramamoorthy, M., Ulbricht, M., 2003. Molecular imprinting of cellulose acetate-sulfonated polysulfone blend membranes for Rhodamine B by phase inversion technique. J. Membr. Sci. 217, 207–214.

Smith, L.E., Rimmer, S., MacNeil, S., 2006. Examination of the effects of poly (*N*-vinylpyrrolidinone) hydrogels direct and indirect contact with cells. Biomaterials 27, 2806–2812.

Stott, P.W., Williams, A.C., Barry, B.W., 2001. Mechanistic study into the enhanced transdermal permeation of a model β-blocker, propranolol, by fatty acids: a melting point depression effect. Int. J. Pharm. 219, 161–176.

Suedee, R., Srichana, T., Chotivatesin, R., Martin, G.P., 2002a. Stereoselective release behaviors of imprinted bead matrices. Drug Dev. Ind. Pharm. 28, 547–556.

Suedee, R., Srichana, T., Martin, G.P., 2000. Evaluation of matrices containing molecularly imprinted polymers in the enantioselective-controlled delivery of β-blockers. J. Contr. Release 66, 135–147.

Suedee, R., Srichana, T., Rattananont, T., 2002b. Enantioselective release of controlled delivery granules based on molecularly imprinted polymers. Drug Del. 9, 19–30.

Torres-Lugo, M., Garcia, M., Record, R., Peppas, N.A., 2002. Physicochemical behavior and cytotoxic effects of p(methacrylic acid-g-ethylene glycol) nanospheres for oral delivery of proteins. J. Contr. Release 80, 197–205.

Ulbricht, M., 2004. Membrane separations using molecularly imprinted polymers. J. Chromatogr. B 804, 113–125.

Ulbricht, M., Belter, M., Langenhangen, U., Schneider, F., Weigel, W., 2002. Novel molecularly imprinted polymer (MIP) composite membranes via controlled surface and pore functionalizations. Desalination 149, 293–295.

Yoshikawa, M., Murakoshi, K., Kogita, T., Hanaoka, K., Guiver, M.D., Robertson, G.P., 2006. Chiral separation membranes from modified polysulfone having myrtenal-derived terpenoid side groups. Eur. Polym. J. 42, 2532–2539.